

Sim-to-Real Learning of Robust Compliant Bipedal Locomotion on Torque Sensor-Less Gear-Driven Humanoid

Shimpei Masuda, Kuniyuki Takahashi

Abstract—In deep reinforcement learning, sim-to-real is the mainstream method as it needs a large number of trials, however, it is challenging to transfer trained policy due to *reality gap*. In particular, it is known that the characteristics of actuators in leg robots have a considerable influence on the *reality gap*, and this is also noticeable in high reduction ratio gears. Therefore, we propose a new simulation model of high reduction ratio gears to reduce the *reality gap*. The instability of the bipedal locomotion causes the sim-to-real transfer to fail catastrophically, making system identification of the physical parameters of the simulation difficult. Thus, we also propose a system identification method that utilizes the failure experience. The realistic simulations obtained by these improvements allow the robot to perform compliant bipedal locomotion by reinforcement learning. The effectiveness of the method is verified using a actual biped robot, ROBOTIS-OP3, and the sim-to-real transferred policy archived to stabilize the robot under severe disturbances and walk on uneven terrain without force and torque sensors.¹

I. INTRODUCTION

If robots can walk on bipedal legs, they can traverse various environments such as slopes, uneven roads, and stairs. In order to achieve this mission, it is important for robots to be robust against disturbances and various environments. As approaches to improve the robustness of legged robots, research based on torque control and the use of compliance have been actively researched in recent years [1]–[3]. Robots that require high power joints, such as those represented by the human full-scale humanoids, are often equipped with gears with high reduction ratios in order to provide output torque while downsizing the actuators. In addition, since installing a torque sensor would increase the cost of the actuator, a configuration that uses a high reduction ratio gear but does not have a joint torque sensor is still a popular option [4]–[6]. Such actuators have elements that are difficult to model, especially represented by gear friction. This friction is difficult to compensate for by the torque controller with joint-level feed-forward compensation, and the ideal output may not always be achieved. Generally, it is complicated to manually design a controller that can work with these considerations.

Deep reinforcement learning (DRL) is being established as a method for developing high-performance robot controllers [7]–[9]. Since DRL requires a large number of trials, the sim-to-real approach, in which policies trained

All authors are associated with Preferred Networks, Inc. {masuda, takahashi}@preferred.jp

¹An accompanying video is available at the following link:
<https://youtu.be/fZWQq9yAYew>

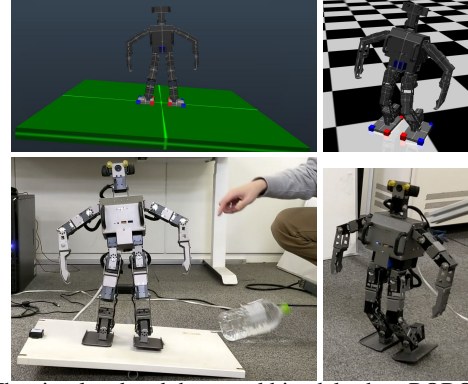


Fig. 1: The simulated and the actual bipedal robot, ROBOTIS-OP3, trained to achieve balancing control under disturbance and walking on uneven terrain without any force/torque sensor.

using simulations are transferred to a real-world robot, has been attracting attention [10]–[12]. In addition, training with simulation is considered to be more promising because it can add various disturbances, try unusual cases, and it does not break robots. However, there are differences in behavior between the simulation and the real environment, commonly referred to as *reality gap*, which prevents the policies trained on the simulation from working in the real environment. Especially for legged robots, it has been reported that the model of the actuators has a considerable influence on the *reality gap* [10], [13], [14]. Furthermore, the instability of the bipedal locomotion causes the sim-to-real transfer to fail catastrophically, making the parameters of an appropriate simulation model, called **system identification**, difficult.

In this study, we propose 1) an actuator model in simulation and a sim-to-real method that can be adapted to robots with torque sensor-less and high reduction ratio geared actuators and 2) a new system identification method that utilizes the failure experience when sim-to-real transfer fails, and realize robust bipedal locomotion, balancing and walking, using DRL.

II. RELATED WORK

A. Joint control in RL for legged robots

When using RL for tasks such as walking and balancing, how to design the policy's actions is one of the focuses. Compared to torque control and velocity control, joint position control improves the efficiency of learning and performance [15]. In recent years, many researches have employed a design in which a position control system is embedded in each joint and the policy outputs the target joint angle as an action, because it is effective [11], [14]. In these studies, the

gain of the joint position control system is fixed, but some studies include the gain in the action [16]. In a joint position control system that converges strongly to the target joint angle, although there is a variation of characteristics in the target tracking behavior, the control error against factors such as friction and load is suppressed, which is advantageous from the viewpoint of *reality gap*, which will be discussed in the next section. However, joint position control with high gain alone is not enough to deal with disturbances and environmental recognition errors caused by noise in the sensor information by robustness based on passivity [1]–[3]. Therefore, in order to enhance the learning efficiency and performance of the RL while making it controllable that joint compliance, this study adopts a variable gain PD that can be selectable up to a low gain. It becomes a challenge to ensure that the torque can be applied accurately, and more precise modeling and joint control are required. Our proposed method addresses these issues by approximate modeling a high reduction ratio gears and introducing it into the simulation.

B. Sim-to-real RL for Robotics

It is widely known that controllers trained by RL in simulations do not work well in actual robots due to *reality gap*, and various approaches have been developed to overcome this challenge. As one of the approaches to sim-to-real, a formulation of the problem of identifying the values of various parameters such as the weight of the robot and the friction of the joints that characterize the simulation behavior (dynamics), has been proposed [12], [17]. Another approach to sim-to-real that has been widely used is domain randomization [18]. This is a method of training a policy by randomly selecting various parameters of the simulation in a certain distribution. Note that for each of the above methods to work effectively, there must be a combination of simulation parameters that can adequately simulate real-world behavior. When the usual combination of friction and inertia parameters is not enough to simulate real-world behavior, it is necessary to add elements to the simulation to reduce the *reality gap*.

In this research, we proposed a method for approximate modeling of high reduction ratio gears. In addition, for tasks with unstable nature where a slight difference in action can easily cause a fall such as bipedal walking, sim-to-real on a real-world robot can lead to catastrophic instability of the results, and it may be difficult to update the simulation parameters using conventional identification methods. Therefore, in this study, we propose a system identification method that uses the failure experience of the sim-to-real procedure.

C. Modeling Actuators in Sim-to-Real Learning

The *reality gap* is a very serious problem that prevents sim-to-real, and this problem is especially critical for actuators in legged robots. To address these challenges, several researches have been conducted to improve the actuator models in the simulation for learning, which can be broadly classified into two categories.

1) Without assuming a model of the actuator, train a neural network to model the behavior of the actuator in part or in whole. For example, a single actuator can be detached from a robot and a neural network can be used to learn the actuator behavior [13], or a small neural network can be used to learn a model that outputs a PD gain that reproduces the torque generated in the actual robot based on the target angle error and angular velocity situation [10].

2) Methods to design a detailed model of the actuator and add it to the simulation. For example, model the DC motor and control latency [11], and model the additional gear backlash [19]. To deal with modeling errors, random noise is added to the output of the actuator in the simulation to absorb the unmodeled elements [14]. However, if there are large differences in the behavior of the actuator between the simulation and the real, it is necessary to increase the noise, which makes it difficult to learn the control policy.

The first method approximates the actuator model by using the high representation power of neural networks, but it requires a huge number of data from actual actuator. In the case of a position control system with variable gain, the required amount of data increases even more when the state space increases depending on the gain as well as the target position, and the behavior is also expected to change depending on the load conditions. Furthermore, it can be difficult to detach the actuator from the robot to obtain data. In this study, we extend the category 2) to model actuators with high reduction ratio gears with low-dimensional parameters based on the characteristics of actuators. We then take an approach that expects the actuator model to be widely generalized in the joint state space, even with parameters identified from a small number of real robot data.

III. PRELIMINARY OF RL

Let $(S, A, T, R, \gamma, s_0)$ be a Markov decision process with state $s \in S$, action $a \in A$, transition probability $T(s_{t+1}|s, a)$, reward function $R(s, a) \in \mathbb{R}$, discount factor $\gamma \in [0, 1]$, and initial state distribution s_0 . RL typically learns a policy $\pi : S \rightarrow A$ to maximize the expected discounted accumulated reward $J = \mathbb{E}[R_t]$ from the initial state, where $R_t = \sum_{i=t}^T \gamma^{(i-t)} R(s_i, a_i)$. This time, the state transition is a transition from control timing t to $t+1$ in a physical simulation or in the real world. S corresponds to the sensor data and A to the commands to the joint actuators. Although various RL algorithms have been proposed, in this study we use Soft-Actor-Critic [20], which supports continuous action spaces and has been reported to have high performance.

IV. METHOD

This method consists of the following three phases. Phase 1: System identification of the simulation parameters so that the real-world robot motion and the simulation motion match in the exciting motion, such as squatting motion. Phase 2: Using the identified simulation parameters, train the RL policy using physics simulation includes proposed actuator model, and apply the trained policy to the actual robot. Phase 3: If the actual robot does not work well

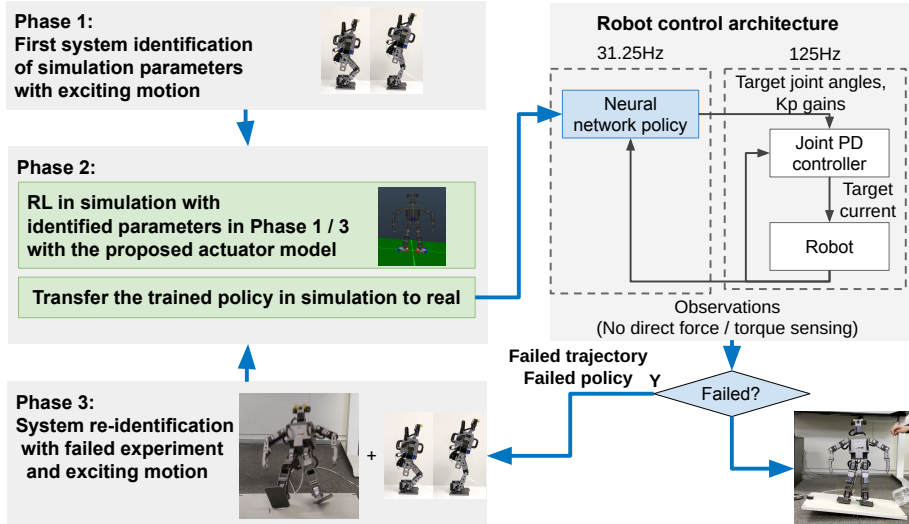


Fig. 2: Concept of the proposed methods. The method consists of the following three phases. Phase 1: System identification of the simulation parameters in exciting motions. Phase 2: Learn RL policy using the parameter identified simulation with the proposed actuator model. Phase 3: If the actual robot does not work using trained policy, the simulation parameters are identified again based on the experience of failure. Then, Phase 2 is run again.

with trained policy in simulation, identify the simulation parameters again based on the failure experience. Phase 2 is then executed again.

We first describe the proposed actuator model in section IV-A. Then, the system identification of the simulation is described in section IV-B.1, followed by the system re-identification using the failure experience in section IV-B.2.

A. Actuator Modeling

This section describes the DC motor model (Section IV-A.1), the current controller model (Section IV-A.2), and the gear friction model (Section IV-A.3) in the simulation of an actuator composed of a DC motor, gears, encoder and current controller.

1) *DC Motor Model*: For the DC motor model, we use the commonly used model [11], which is represented by the following equation:

$$\begin{aligned} \tau &= K_t I \\ I &= \frac{V_{pwm} - V_{back-emf}}{R} \\ V_{back-emf} &= K_t \dot{q} \end{aligned} \quad (1)$$

where, τ is the exerted torque by the motor, I is the current, K_t is the torque constant of the motor, R is the terminal resistance, V_{pwm} is the voltage applied to the motor, $V_{back-emf}$ is the induced electromotive force, and \dot{q} is the angular velocity of the shaft.

2) *Current Controller Model*: Here, we describe the current controller model. Assuming that the current control is performed with a sufficiently short control period compared to the high-level command frequency, such as the control loop of the robot, and that the inductive electromotive force is compensated, the applied voltage at each simulation time step can be formulated by the following equation:

$$\begin{aligned} V_{pwm}^{targ} &= RI^{targ} + V_{back-emf,t} \\ V_{pwm} &= CLIP(V_{pwm}^{targ}, -V_{battery}, V_{battery}) \end{aligned} \quad (2)$$

where, I^{targ} is the target current and $V_{back-emf,t}$ is the induced electromotive force based on the current angular velocity. Since the target voltage, V_{pwm}^{targ} , is limited by the battery voltage $V_{battery}$, the target current is not output when the angular velocity is large. It is difficult to perfectly compensate for induced electromotive force in actual actuators, and it is considered that there are errors at the microscopic level. In this study, we assume that they are represented by other model components, and expect to obtain parameters that are consistent with the overall behavior in the system identification described in Section IV-B. For example, a constant lack of compensation of the induced electromotive force would be represented by an increase in viscous friction, while an excess of compensation would allow the macroscopic behavior to be matched by increasing the torque constant or reducing the rotor inertia.

3) *Gear Friction Model*: Here, we describe a gear friction model. In this study, a general friction model and a friction model specific to high reduction ratio gears are used together. This is because the nature of the two frictions are different: general friction is frictional loss dependent on angular velocity, while gear efficiency is frictional loss dependent on force. First, the Stribeck friction τ_{fric} is used as the general friction model by the following equation:

$$\begin{aligned} s &= \frac{\exp(|\dot{q}|)}{\dot{q}_{static}} \\ \tau_{fric} &= f_s + s(f_s - f_c) + k_v |\dot{q}| \end{aligned} \quad (3)$$

where, each parameter f_s , f_c , k_v , and \dot{q}_{static} are the static friction force, the Coulomb friction coefficient, the viscous friction coefficient, and the angular velocity value regarded as non-static, respectively.

For high reduction ratio gears, there is an asymmetry in transmission efficiency depending on the drive direction [21], [22]. In order to implement this directional efficiency precisely, it needs to be taken into consideration in the optimization process that iterates the physical simulation. In

this work, we implement an approximate model in which the force loss due to this transfer efficiency is denoted as an additional brake torque applied to the joint in the simulation. Using the forward and backward transmission efficiencies as parameters, respectively, the brake torque, which varies at each time depending on the torque generated by the motor or the load applied to the joint, is calculated. Assuming that the motion of the robot is quasi-static and the load on each joint varies continuously in the physical simulation, the brake torque for each simulation step is calculated by the following equation:

$$f(\tau_m, \tau_a, \eta_{fw}, \eta_{bw}) = \begin{cases} -L_{fw} & \text{if } \text{sign}(\eta_{fw}\tau_m + \tau_a) = \text{sign}(\tau_m) \\ -L_{bw} & \text{if } \text{sign}(\tau_m + \eta_{bw}\tau_m) = \text{sign}(\tau_a) \\ -(\tau_m + \tau_a) & \text{else} \end{cases} \quad (4)$$

where, $L_{fw} = (1 - \eta_{fw})\tau_m$, $L_{bw} = (1 - \eta_{bw})\tau_a$

where, τ_m is the generated torque from the motor, τ_a is the load torque on the joint, and η_{fw} and η_{bw} are the forward and backward transmission efficiencies, respectively. The torque generated by the motor is amplified by the gear reduction ratio. When τ_m is clearly greater than τ_a or the directions of τ_m and τ_a are the same, it is regarded as a forward drive state and the brake torque based on the forward transmission efficiency is generated. If the directions of τ_m and τ_a are opposite and τ_a is larger even after considering the backward direction efficiency, it is considered to be in the backward drive state and the brake torque based on the backward direction transfer efficiency is generated. A state that does not meet either conditions is an antagonistic state with no apparent difference between τ_m and τ_a , and thus generates a brake torque such that $\tau_m + \tau_a + \tau_{brake} = 0$. Since τ_a is approximated using the value of the current simulation state, there is a concern that the simulation may become unstable, however, it is reasonably expected to be stable when used in conjunction with the Stribeck friction described above.

B. System Identification for Sim-to-real

This section describes the system identification method of the simulation parameters, such as the parameters of the actuator model shown in Section IV-A.

1) *System Identification of Simulation Parameters*: Computing simulation parameters with black-box optimization [10], [23] so as to match the observed results on the actual robot with the observed results on the simulation in similar motions is suitable for sim-to-real learning due to the following advantages: 1) The simulation can be improved from the results of the actual robot alone without detaching the actuator from the robot, and 2) the simulation can be optimized by reproducing the behavior of the actual robot as the objective function.

First, a suitable exciting motion for system identification is designed as time series data θ^{targ} of the target angle of each joint. The exciting motion used in this study will be described in section V-B. A simple position control feedback system is provided to track θ^{targ} in the actual robot. We then collect a set of sensor information \mathbf{O}^{real} for the robot in motion. This

sensor information includes the angle of each joint, angular velocity, current and the tilt of the upper body. Similarly, on the physical simulation built based on the parameter group ϕ , the same position control feedback system is used to perform the motion to track θ^{targ} and obtain \mathbf{O}^{sim} . The parameter ϕ that minimizes the difference between \mathbf{O}^{real} and \mathbf{O}^{sim} is calculated by sampling-based black-box optimization as follows:

$$\min_{\phi} L(\mathbf{O}^{\text{sim}}(\phi, \theta^{\text{targ}}), \mathbf{O}^{\text{real}}(\theta^{\text{targ}})) \quad (5)$$

Even if the simulation parameter ϕ that can simulate the robot's behavior in a specific trajectory is identified, there is still a possibility that there is the *reality gap* when the policy performs the task on the actual robot. Domain randomization has been used frequently in sim-to-real research to increase the robustness of the policy so that the task can be achieved even in the presence of *reality gap*, and we also use in this study. Domain randomization [18] is a method to improve robustness by randomizing the physics parameters of the simulation within a specific range during RL training, thereby preventing the policy from over-fitting to a specific environment.

2) *System Identification from Failure Experience*: When the trained policy with simulation that improved by the approaches described in section IV-B.1 is executed on the actual robot, it sometimes does not work catastrophically. For example, the actual robot may not even be able to stand on flat ground if a policy that has been trained to balance on two legs against disturbances in a simulation is applied to the actual robot. In this paper, we propose a method to use this failure experience due to *reality gap* to re-identify the simulation parameters. In such a failure case, the control of the actual robot by the policy is oscillatory, and the joint angle trajectory of the actual robot differs greatly due to small differences in the initial posture and other factors. It is difficult to make comparisons in joint angles, etc. for each time series in the same way as equation (5). Therefore, in order to abstractly extract the behavior that the robot became oscillatory and fell down, we use the cumulative reward obtained from the real robot. Then, we use the difference between the expected in real and the cumulative reward obtained from the policy behavior in the new parameter candidate for evaluation. Assume that the rewards include elements corresponding to the features of the motion, such as time until fall based on survival rewards or joint angular velocity penalties.

Due to the influence of domain randomization and the robustness acquired in the RL process itself, or due to the lack of elements in the simulation model, it may not be possible to get sufficient failure motions of the actual robot even if the parameters are drastically changed in the simulation. Therefore, we introduce an additional disturbance in the simulation to induce the failure motion. For example, a large noise to the IMU sensor input can be used. By penalizing according to the magnitude of this unknown disturbance and by optimizing the difference in the reward of the policy action along with the error of the exciting

TABLE I: List of parameters for system identification

Parameter	Unit	Range
motor Kt	-	[0.003, 0.009]
motor R	Ω	[4.0, 9.0]
motor armature	kgm^2	[0.003, 0.011]
gear backward efficiency	-	[0.6, 1.0]
joint f_c	Nm	[0.01, 0.25]
joint k_v	-	[0.0025, 0.15]
joint f_s	Nm	$f_c + [0.0, 0.25]$
base mass offset	Kg	[0.0, 0.5]
base CoM offset x	m	[-0.02, 0.02]
base CoM offset z	m	[-0.02, 0.02]

motion in equation (5), we can obtain the parameters of the simulation that will cause the policy to fail while keeping the error in the exciting motion as small as possible. When the reward R of the actual robot is obtained as a result of running the policy π that was trained using the parameter ϕ , the new parameter is estimated by the following optimization equation:

$$\begin{aligned} \min_{\phi, \mathbf{D}} \quad & L(\mathbf{O}^{sim}(\phi, \theta^{targ}), \mathbf{O}^{real}(\theta^{targ})) \\ & + \|E[R^{real}(\pi)] - E[R^{sim}(\phi, \mathbf{D}, \pi)]\|^2 + \|\mathbf{D}\|^2 \end{aligned} \quad (6)$$

where, $E[R^{real}(\pi)]$ is the expected value of the actual robot reward, $E[R^{sim}(\phi, \mathbf{D}, \pi)]$ is the reward as a result of running the policy in the simulation, and \mathbf{D} is the disturbance parameter. Using the parameters of the simulation obtained by this method, RL can be performed again, which is expected to improve the performance of the actual robot.

V. EXPERIMENTAL SETUP

A. Robot Setup: ROBOTIS-OP3

In this study, ROBOTIS-OP3 from ROBOTIS was used as a bipedal robot [24]. ROBOTIS-OP3 has a length of 51 cm, a weight of about 3.5 Kg, 6-DOFs in each leg, and 20-DOFs in total (Fig. 1). The control is executed in 125 Hz. In each control step, commands are send to each joint servo motor, the servo states are received, and IMU information is obtained. Servo state includes the current joint angle and current value. IMU information includes sensor values of 3-axis gyro, 3-axis accelerometer, and 3-axis magnetometer.

All the joints of the robot are composed of Dynamixel servo motors XM430-W350. The stall torque is 4.1 Nm at 12.0 V and 2.3 A. The gears consists of metal spur gears and has a reduction ratio of 353.5. In addition to general position control commands, a mode that allows direct command of the target current is equipped. In this study, this current control mode is used.

B. System Identification and Domain Randomization

The system identification of the actual robot environment (ROBOTIS-OP3) is conducted by the following procedure. 1) Using the exciting motion, the first system identification is conducted by equation (5). 2) The obtained simulation parameters are used to train the policy by RL. Then, the trained policy is executed on the actual robot. The simulation was implemented using Mujoco [25]. 3) If the performance of the policy is poor, the simulation parameters are re-identified based on the failure experience using equation (6), and the policy is trained again by RL. In this study, we conduct system identification of the parameters shown in

Table II. Note that the motor armature is the additional link inertia caused by the rotor inertia of the DC motor, and was amplified with square of the gear reduction ratio from rotor inertia itself.

For the equation (5) and (6) of the numerical optimization for system identification, we use the Tree-structured Parzen Estimator algorithm implemented in Optuna [26] since it gives better results than CMAES in our experimental setup.

For the exciting motion θ^{targ} for system identification, a simple squatting motion is used. While keeping a forward leaning posture, execute a flexion/extension movement such that the knee joint angle flexes from 1.47 rad to 0.6 rad at a speed of approximately 0.5 Hz. To evaluate the error L from the squatting motion, equation (7) is used. For each time series, take the average of the errors in the position, velocity, and current of each joint, and the tilt and angular velocity of the upper body posture.

$$\begin{aligned} L = & \frac{1}{T} \sum_{t=1}^T (\|r_t^{sim} - r_t^{real}\|^2 + \|\dot{r}_t^{sim} - \dot{r}_t^{real}\|^2) + \\ & \frac{1}{NT} \sum_{t=1}^T \sum_{i=1}^N (\|\theta_{t,i}^{sim} - \theta_{t,i}^{real}\|^2 + \|\dot{\theta}_{t,i}^{sim} - \dot{\theta}_{t,i}^{real}\|^2 + \|I_{t,i}^{sim} - I_{t,i}^{real}\|^2) \end{aligned} \quad (7)$$

As a method to deal with the *reality gap*, domain randomization is applied during RL. Random selection is applied only to the IMU noise, and for each episode the noise is given uniformly at random in the following range: Gyro offset is $[-0.2, 0.2]$, gyro ratio is $[0.75, 1.25]$, acceleration offset is $[-1.5, 1.5]$. The IMU information of the policy observation will be $Gyro_{obs} = (Gyro_{sim} + Gyro_{offset}) \times Gyro_{ratio}$ and $Acc_{obs} = Acc_{sim} + Acc_{offset}$.

C. Task for Evaluation

We describe the evaluation task: 1) balancing task during standing upright under disturbance in section V-C.1, and 2) walking task in section V-C.2. Note that we use fully-connected neural network for the policy training of both tasks. The networks have 3 hidden layers with ReLU activation and each layer has 256 nodes.

1) *Balancing task:* In this section, we describe balancing task during standing upright in environments with disturbances. The objective is to have the robot balance during standing upright on a board with dynamically changing tilt, and to have the robot keep its posture without falling over even with a sudden change in floor tilt (Fig. 1).

The action of the policy in this RL is the target angle and P gain of PD control for each joint. Each joint command of the robot is calculated based on the action, using $\theta_{PD}^{targ} = \theta^{ref} + \Delta_\theta a_\theta$ for the target joint angle and $K_p = K_p^{ref} + \Delta_{K_p} a_{K_p}$ for the P-gain. Where, θ^{ref} is the reference joint angle of the standing posture, Δ_θ is the joint angle width, a_θ is the action corresponding to the target angle, Δ_{K_p} is the gain width, a_{K_p} is the action corresponding to the gain, and the D-gain is fixed to 0.1. The target joints are five for each leg except for the yaw axis, for a total of 10 joints for both legs, and the action space has 20 dimensions of $[-1, 1]$. For the balancing task, we experimentally set $\Delta_\theta = 0.3$ and $\Delta_{K_p} = 2.5$. The

observation of RL policy in this task includes the following elements:

- The position and velocity of the 9 keypoints placed on the legs and upper body with the base link as the origin (54 dims)
- Target angle and K_p gain of PD control for each joint commanded in the previous step (20 dims)
- Angular velocity of base link excluding yaw axis (2 dims)

For the observation of the keypoints of each part of the robot with reference to [27], each joint angle and angular velocity are mapped in space along with the base link posture, and the keypoints include the center of the neck link, the knee center of each foot, the three corners of each sole plates. In order to be aware of the time series of the state, we concatenate the above observation obtained in the previous step with the observation obtained in the latest step then feed to the policy. The total number of dimensions of observation is 152. The reward function is calculated by subtracting scores from the survival reward by each penalty terms include the following elements: the difference from the reference posture, the magnitude of the joint angular velocity, the distance of the base link position from the reference point, the tilt of the base link, the angular velocity of the base link, the magnitude of the joint current, and the distance from the action of the previous step. The disturbance is given to the board by causing it to vibrate at random amplitudes and frequencies during each episode. The amplitude is up to 10° in the direction of the robot roll axis and up to 4° in the direction of the pitch axis. The frequency is set in the range $[0.25, 1.0]$ Hz and the vibration is determined independently for the roll and pitch axes.

2) *Walking task*: In this section, we describe the walking task. The bipedal walking task is an advanced task that requires more active motion than the balancing task. The objective is to walk forward on a flat surface at a constant speed (Fig. 1). The action space for the RL task is the same as in the balancing task described in section V-C.1, but the ΔK_p is increased to 4.5 to account for the possibility of needing to exert a strong torque in some situations. The observation space is also the same as in the balancing task, but with the addition of periodic signals of walking encoded in two dimensions. The reward function is designed similarly to the prior study by Siekmann *et al.* [16], so refer to their paper for details. The penalty terms of the reward included the difference from the target velocity, the floor reaction force in the swing leg and the toe velocity in the supporting leg, the base link posture difference from the target posture, the acceleration and angular velocity of the base link, the magnitude of the joint current, and the distance to the action of the previous step. The target walking cycle was set at 1.0 sec, and the ratio of the support leg phase to the swing leg phase was set at 0.7 : 0.3.

VI. RESULTS

In this experiment, the following three points are evaluated to verify the effectiveness of the proposed method.

TABLE II: Results of system identification

Parameter	Squat model	w/ gear model	w/o gear model	Tuned
Standing succeeded	✗	✓	✓	✓
motor Kt	0.0066	0.0063	0.0077	0.006
motor R	4.00	6.42	4.81	7.2
motor armature	0.0083	0.0032	0.0041	0.0035
gear backward efficiency	0.63	0.79	1 (Fixed)	0.62
joint f_c	0.10	0.028	0.036	0.02
joint k_v	0.011	0.048	0.037	0.015
joint f_s	0.11	0.037	0.036	0.025
base mass offset	0.48	0.099	0.23	0.4
base CoM offset x	0.0023	0.00076	0.00027	0.0
base CoM offset z	0.017	0.019	0.018	0.0

- Validation of the proposed system identification method for sim-to-real (section VI-A)
- Verification of the effectiveness of gear model for sim-to-real (section VI-B)
- Verifying the robustness of trained policies to disturbances (section VI-C & section VI-D)

A. Evaluation of System Identification Method

The system identification method was evaluated by experiments to identify the simulation parameters that enable the sim-to-real transfer of policy. First, the parameters of the system identification obtained when using only the squatting motion as the exciting motion according to equation (5) as the baseline are shown in Squat model of Table II. As a result of learning policy for the balancing task using the Squat model and executing sim-to-real transfer, the robot could not even keep a standing posture on a flat surface with the actual robot. Next, following equation (6), the results of the system re-identification using the falling experience are shown in w/ gear model of Table II. As a result of re-training policy for the balancing task and executing sim-to-real transfer using the w/ gear model, the robot was able to keep a standing posture on the actual robot. In addition, we performed the system re-identification without the proposed gear model of the actuator, which also successfully kept a standing posture on the actual robot (w/o gear model in Table II). These results demonstrate that the *reality gap* was reduced by system re-identification.

Experimental adjustments were made based on the small motor armature of less than 0.004, the backdrive efficiency of less than 80%, and the tendency for small friction obtained from the results of system identification for the squatting motion alone. Then, we found simulation parameters that provide a more stable sim-to-real transfer than the w/ gear model. The results are shown as Tuned in Table II, and these simulation parameters were used in the later experiments.

In our experiments, we confirmed that the common characteristic of the simulation parameters that were successfully transferred to the actual robot by sim-to-real was that the armature value was smaller than the reasonable value for DC motors of the same size. The internal motor specifications of XM430-W350 are not publicly available, but based on similar-sized DC motors with publicly available specifications and a gear reduction ratio of 353.5, the armature value is generally expected to be around 0.01 kgm^2 . For this result, we suspect that the motor behavior caused by the error during current control is expressed as a decrease in armature.

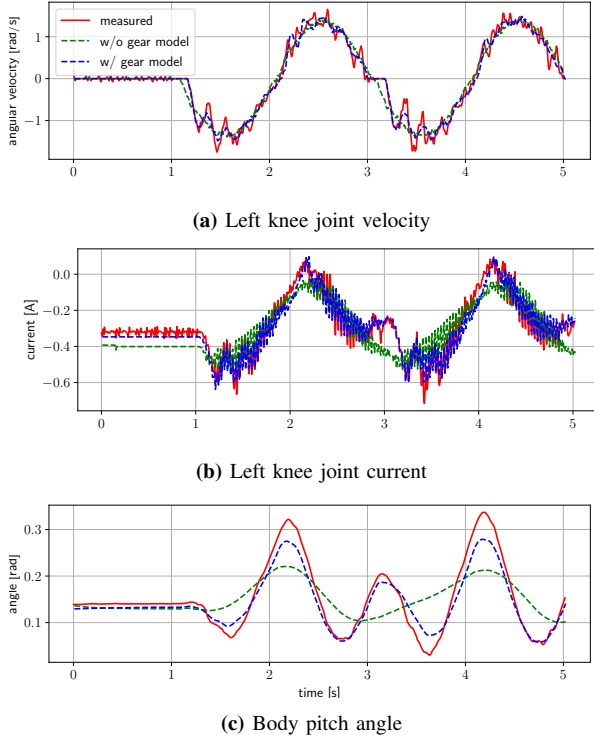


Fig. 3: Result of system identification with squat motion.

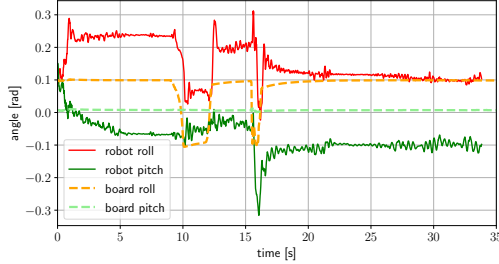


Fig. 4: Sensor measurements of balancing task.

B. Evaluation of Actuator Modeling

We conducted experiments to evaluate the effectiveness of the gear model. First, we describe the details of the system identification results for the squatting motion. Using equation (5), system identifications with and without the addition of the gear model were performed. The error evaluation was based on equation (7), and the error scores of the optimization results were 0.038 with the gear model and 0.069 without the gear model. Fig. 3 shows the graphs showing the information of the actual robot and the simulated robot during the squatting motion. We can confirm quantitatively that there is an improvement not only in the error score but also in the joint angular velocity and upper body posture.

Next, we describe the effect of the gear model on the sim-to-real transfer. Using the w/o gear model and the Tuned model shown in section VI-A, we performed the training of the balancing task and the walking task in simulation and, then, transfer it to the actual robot. In the balancing task, we applied the disturbances as verified in the next section (section VI-C for details), but we could not see a clear performance difference between the w/o gear model

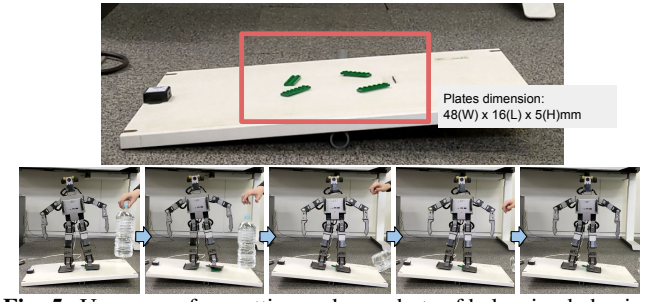


Fig. 5: Uneven surface setting and snapshots of balancing behavior.

and the Tuned model. In the walking task, only the Tuned model was able to walk on the actual robot. Considering the instability of the RL results, the w/o gear model was trained using five seed values, but none of them resulted in walking on the actual robot. On the other hand, the Tuned model successfully walked with 2 seeds out of a total of 5 seeds. From this result, we can say that the walking task was successfully performed on the actual robot in sim-to-real transfer due to the reduction of the *realy-gap* by using the gear model.

C. Balancing Experiment

In order to verify the robustness of the trained policy to disturbances, we evaluated the performance of the trained policy for the balancing task when transferred to the actual robot. First, we describe the disturbance tolerance on a flat board similar to the simulation environment. A board which tilts from -6° to 6° was prepared and disturbance was given to the board while the actual robot was controlled by the trained policy. The disturbance was given by the impact of a weight of about 1 Kg falling to the edge of the board. The first impact was applied at around 10 sec in Fig. 4, and the second impact was applied at around 15 sec. Especially in the second disturbance, the board changed its angle in a short time, but the robot stabilized its posture without falling over.

Next, we evaluated the disturbance tolerance when the the surface of the board was uneven. Although the surface of the board was always flat during training in simulation, if the policy is flexible enough to change the gain of PD control without unnecessarily increasing it, and if it is passive to the environment, it is expected to be able to cope with uneven surfaces by adjusting its balancing action. Fig. 5 shows the experimental environment with unevenness added to the board surface and the overall behavior when a disturbance is applied. It was confirmed that the stabilization control was achieved even on an unknown ground shape, and the robot could keep an upright posture (Bottom part of Fig. 5).

D. Walking Experiment

In order to verify the robustness of the trained policy to disturbances, we evaluated the performance of the trained

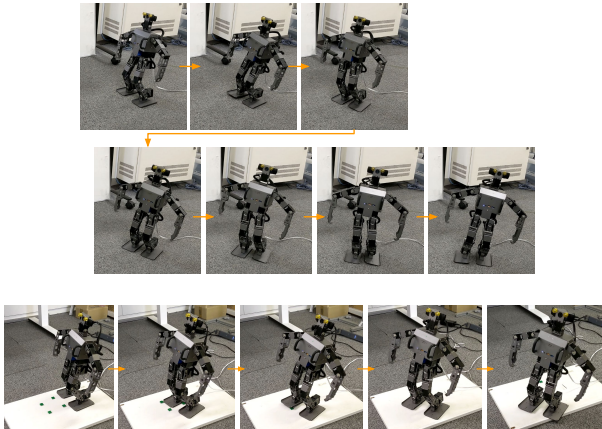


Fig. 6: Snapshots of walking experiments on flat surface and uneven surface.

policy for the walking task when transferred to the actual robot. First, we evaluated the walking motions on the same flat surface as in the simulation. The upper and middle part of Fig. 6 shows a snapshot of the walking motion on flat surface. It was confirmed that the robot controlled its center of gravity appropriately and moved forward. It is not good in terms of straightness, stride, and swinging of the swing leg, which is similar to the RL results in the simulation, and the RL process needs to be improved.

Next, we investigated the walking motion on uneven surfaces. As mentioned in the balancing task experiment (section VI-C), if the robot has passivity due to variable gain, it can be expected to cope with unknown uneven surfaces. The results of walking motion on an uneven terrain are shown in the bottom part of Fig. 6. The size of four green blocks in the figure is about $16(W) \times 16(L) \times 5(H)$ mm. Even though the robot is not equipped with a foot force sensor, it was able to run across the uneven surface. This result supports the fact that the toe force and torque can be output with sufficient accuracy and is equivalent to the simulation, and that the policy utilizes soft control with variable gain, rather than hard position control, in the walking task.

VII. CONCLUSION

In this paper, we propose a method to acquire robust control policy of the actual robot by RL, using a model of a high reduction ratio gears and a system identification method that utilizes the experience of failed sim-to-real transfers. The method was verified on the actual robot, ROBOTIS-OP3, and achieved balancing control under disturbance and walking on uneven terrain without any force/torque sensor.

REFERENCES

- [1] S. Hyon and G. Cheng, “Passivity-based full-body force control for humanoids and application to dynamic balancing and locomotion,” in *2006 IEEE/RSJ International Conference on Intelligent Robots and Systems*, 2006, pp. 4915–4922.
- [2] G. Mesesan, *et al.*, “Dynamic walking on compliant and uneven terrain using dcm and passivity-based whole-body control,” in *2019 IEEE-RAS 19th International Conference on Humanoid Robots (Humanoids)*, 2019, pp. 25–32.
- [3] H. Suzuki, *et al.*, “Torque based stabilization control for torque sensorless humanoid robots,” in *2017 IEEE-RAS 17th International Conference on Humanoid Robotics (Humanoids)*, 2017, pp. 425–431.
- [4] K. Kaneko, *et al.*, “Humanoid robot hrp-5p: An electrically actuated humanoid robot with high-power and wide-range joints,” *IEEE Robotics and Automation Letters*, vol. 4, no. 2, pp. 1431–1438, 2019.
- [5] K. Kojima, *et al.*, “Development of life-sized high-power humanoid robot jaxon for real-world use,” in *2015 IEEE-RAS 15th International Conference on Humanoid Robots (Humanoids)*, 2015, pp. 838–843.
- [6] ROBOTIS CO.,LTD, “THORMANG3 INTRODUCTION,” <https://emanual.robotis.com/docs/en/platform/thormang3/introduction/> (accessed on 27 Feb 2022).
- [7] J. Lee, *et al.*, “Learning quadrupedal locomotion over challenging terrain,” *Science Robotics*, vol. 5, no. 47, Oct 2020. [Online]. Available: <http://dx.doi.org/10.1126/scirobotics.abc5986>
- [8] J. Siekmann, *et al.*, “Blind bipedal stair traversal via sim-to-real reinforcement learning,” <https://arxiv.org/abs/2105.08328>, 2021.
- [9] X. B. Peng, *et al.*, “Learning agile robotic locomotion skills by imitating animals,” in *Robotics: Science and Systems*, 07 2020.
- [10] W. Yu, *et al.*, “Sim-to-real transfer for biped locomotion,” in *2019 IEEE/RSJ International Conference on Intelligent Robots and Systems (IROS)*, 2019, pp. 3503–3510.
- [11] J. Tan, *et al.*, “Sim-to-real: Learning agile locomotion for quadruped robots,” 2018. [Online]. Available: <https://arxiv.org/abs/1804.10332>
- [12] Y. Du, *et al.*, “Auto-tuned sim-to-real transfer,” in *2021 IEEE International Conference on Robotics and Automation (ICRA)*, 2021, pp. 1290–1296.
- [13] J. Hwangbo, *et al.*, “Learning agile and dynamic motor skills for legged robots,” *Science Robotics*, vol. 4, no. 26, Jan 2019. [Online]. Available: <http://dx.doi.org/10.1126/scirobotics.aa5872>
- [14] Z. Xie, *et al.*, “Learning locomotion skills for cassie: Iterative design and sim-to-real,” in *Proceedings of the Conference on Robot Learning*, ser. Proceedings of Machine Learning Research, vol. 100, 2020, pp. 317–329.
- [15] X. B. Peng and M. van de Panne, “Learning locomotion skills using deeprl: Does the choice of action space matter?” in *Proceedings of the ACM SIGGRAPH/Eurographics Symposium on Computer Animation*, ser. SCA ’17, 2017, pp. 12:1–12:13.
- [16] J. Siekmann, *et al.*, “Sim-to-real learning of all common bipedal gaits via periodic reward composition,” in *2021 IEEE International Conference on Robotics and Automation (ICRA)*, 2021, pp. 7309–7315.
- [17] Y. Chebotar, *et al.*, “Closing the sim-to-real loop: Adapting simulation randomization with real world experience,” in *2019 International Conference on Robotics and Automation (ICRA)*, 2019, pp. 8973–8979.
- [18] J. Tobin, *et al.*, “Domain randomization for transferring deep neural networks from simulation to the real world,” <https://arxiv.org/abs/1703.06907>, 2017.
- [19] M. Taylor, *et al.*, “Learning bipedal robot locomotion from human movement,” in *2021 IEEE International Conference on Robotics and Automation (ICRA)*, 2021, pp. 2797–2803.
- [20] T. Haarnoja, *et al.*, “Soft actor-critic: Off-policy maximum entropy deep reinforcement learning with a stochastic actor,” <https://arxiv.org/abs/1801.01290>, 2018.
- [21] A. Wang and S. Kim, “Directional efficiency in geared transmissions: Characterization of backdrivability towards improved proprioceptive control,” in *2015 IEEE International Conference on Robotics and Automation (ICRA)*, 2015, pp. 1055–1062.
- [22] H. Matsuki, *et al.*, “Bilateral drive gear—a highly backdrivable reduction gearbox for robotic actuators,” *IEEE/ASME Transactions on Mechatronics*, vol. 24, no. 6, pp. 2661–2673, 2019.
- [23] J. Tan, *et al.*, “Simulation-based design of dynamic controllers for humanoid balancing,” in *2016 IEEE/RSJ International Conference on Intelligent Robots and Systems (IROS)*, 2016, pp. 2729–2736.
- [24] ROBOTIS CO.,LTD, “ROBOTIS-OP3 INTRODUCTION,” <https://emanual.robotis.com/docs/en/platform/op3/introduction/> (accessed on 27 Feb 2022).
- [25] E. Todorov, *et al.*, “Mujoco: A physics engine for model-based control,” in *2012 IEEE/RSJ International Conference on Intelligent Robots and Systems*, 2012, pp. 5026–5033.
- [26] T. Akiba, *et al.*, “Optuna: A next-generation hyperparameter optimization framework,” in *Proceedings of the 25rd ACM SIGKDD International Conference on Knowledge Discovery and Data Mining*, 2019.
- [27] X. B. Peng, *et al.*, “Deeploco: Dynamic locomotion skills using hierarchical deep reinforcement learning,” *ACM Transactions on Graphics (TOG)*, vol. 36, no. 4, pp. 1–13, 2017.